jet INTL JOURNAL OF ELECTRONICS AND TELECOMMUNICATIONS, 2019, VOL. 65, NO. 3, PP. 455-461
Manuscript received May 8, 2019; revised August, 2019. DOI: 10.24425/ijet.2019.129799

Impact of Climatic Conditions to Capacity of Airborne Ultrasonic Channel

Gustaw Mazurek

***Abstract*—In this paper, we estimate the upper limit of the transmission data rate in airborne ultrasonic communications, under condition of the optimal power allocation. The presented method is based on frequency response of a channel in case of single-path LOS propagation under different climatic conditions and AWGN background noise model, and it can be easily extended to the case of frequency-dependent noise. The obtained results go beyond the discrete distances for which experimental SNR values were available, and are more accurate than the previous calculations in the literature, due to the inclusion of the channel frequency response and its changes over the distance. The impact of air temperature, relative humidity and the atmospheric pressure on the channel capacity is also investigated. The presented results can serve as a reference during the design of airborne ultrasonic communication systems operating in the far-field region.**

***Keywords*—Air-coupled ultrasound, digital communication, channel estimation, channel capacity, acoustic data transmission**

I. Introduction

Acoustic and ultrasonic data transmission can be employed in areas where severe attenuation of electromagnetic waves prevents effective RF communication, for example under water [1], through metallic barriers [2], and along drill strings [3] in logging-while-drilling applications. The ultrasonic systems can be applied as an alternative to short-range RF wireless systems where radio emission has to be avoided in areas with equipment sensitive to EMI [4] or when the employment of radio systems is restricted by law. Additionally, ultrasonic communications can offer more secure data transfer when compared to RF systems [5] due to propagation effects.

In recent years, different experimental systems with airborne ultrasonic transmission have been investigated, with indoor wireless communication on a short-range (typically up to 11 m). The most of work in this area was focused on demonstration of a new physical layer for digital communication, selection of optimal frequency band, modulation [6], pulse shaping [5] and coding scheme [7]. However, there is still a need to evaluate the theoretical performance measures for this kind of wireless transmission channel.

A. Related work

The maximum data rate of reliable transmission in a flat AWGN communication channel can be determined according to Shannon-Hartley theorem [8] as

$$C = B\log_2[(P+N_\mathrm{t})/N_\mathrm{t})] = B\log_2(1+\mathrm{SNR}) \qquad (1)$$

G. Mazurek is with Warsaw University of Technology, Institute of Electronic Systems, Warsaw, Poland (e-mail: g.mazurek@elka.pw.edu.pl).

in bits/s, where B is the bandwidth of the channel, P is the average signal power, N_t is the power of white thermal noise and SNR denotes the signal-to-noise ratio. The equation (1) is valid in case of the flat AWGN channel.

The transmission bandwidth B and the theoretical channel capacity C have been evaluated for acoustic and ultrasonic communication channels with different transmission media. In [9], the communication system is presented that consist of two ultrasound contact transducers separated by a 0.25 inch steel plate. The measured bandwidth of such a channel was 2.9 MHz with SNR around 30...40 dB. The upper limit of the channel capacity was expected around 29 Mbit/s. A more advanced system with OFDM transmission through a metallic barrier has been presented in [2], with 63.5 mm block of steel separating two piezoelectric transducers. The channel capacity was estimated around 48 Mbit/s thanks to higher bandwidth (ca. 4 MHz) and SNR (44 dB). Further increase of the system performance has been obtained [10] with applying MIMO-OFDM techniques. The communication system with seven pairs of transducers separated by a 40 mm steel barrier has achieved the theoretical channel capacity around 700 Mbit/s, with half of that value as the practical data rate.

The bandwidth and the theoretical channel capacity in the case of ultrasonic transmission in the human body was evaluated in [11] for wireless biomedical applications. Fundamentals of ultrasonic wave propagation in tissues, reflections, scattering, and possible sources of noise were discussed. Finally, the bandwidth and the capacity were calculated as a function of the propagation distance. The estimated channel capacity has extended from around 100 Mbit/s in long distances (10 cm), up to 30 Gbit/s (0,1 mm).

Performance evaluation of the underwater acoustic communication channel was presented in [12]. With using an analytical method that takes into account physical models of propagation and ambient noise in the ocean, optimal signal energy allocation was calculated that maximizes the channel capacity under the constraint of finite transmission power. Closed-form approximations for the bandwidth, transmission power and the channel capacity (assuming SNR $=$ 20 dB) were derived as a tool for the design and analysis of underwater acoustic networks. In [1], a campaign of measurements of underwater acoustic channels in shallow waters was presented. Results of these measurements were used to determine numerical parameters of the channel model. The theoretical capacity of the channels was evaluated with a closed-form expression. Finally, the channel capacity was estimated around 4 bit/s for each 1 Hz of the bandwidth (assuming SNR=12.5 dB). These results, however, cannot be directly applied to airborne ultrasonic communications due to completely different characteristics of the transmission channel.

In a context of ultrasonic communications in the air, the first estimate of the theoretical channel capacity can be found in [5]. The channel capacity for a system with 350 kHz of effective bandwidth was estimated around 1.3 Mbit/s, assuming $E_b/N_o = 19$ dB and the transmission distance of 1.2 m. More estimates of the theoretical channel capacity in airborne ultrasonic communications have been provided in [13] for several systems with different kind of transducers. These calculations have been based on numerical results from experiments reported in the literature. The obtained results, however, were limited only to a few discrete distances, for which the bandwidth and SNR values were available, and under the assumption of flat channel frequency response and constant bandwidth irrespective of the distance.

The assumption of flat frequency response in [13] may be far from the real conditions. It is known that sound absorption coefficient in air increases with the square of the frequency [14]. As a result, the higher frequencies suffer significant attenuation at longer distances, which must have an impact both to the channel bandwidth and the shape of its characteristics, as has been shown in [15]. Therefore, it is possible to develop a more adequate frequency-dependent channel model for the airborne ultrasonic transmission, and the channel capacity may be estimated more precisely.

The main contribution of this paper is to evaluate the theoretical performance limits of airborne ultrasonic communications for any distance in the far field, without limitations to the discrete points with experimentally determined SNR values. Our estimations are based on the experimental results available in the literature. The results are presented in plots of the channel capacity as a function of the distance as well as a simple analytical expression that can approximate the results of numerical computations. The influence of climatic conditions (i.e. the air temperature, relative humidity and atmospheric pressure) to the channel capacity is also discussed.

II. Ultrasonic channel model

We assume single-path, line-of-sight (LOS) propagation of ultrasound waves in air. The transmitter and receiver transducers are aligned in parallel on the common acoustic axis and separated by the distance d. In such conditions we can expect three main factors [16] affecting the channel frequency response: ultrasonic absorption in the air, spatial field response and transducer frequency response. The assumed propagation scenario can be applied to a few practical situations, for example, when the transducers are working in fixed positions in a relatively big room, when there are no obstacles and all reflected signals can be neglected due to their low power level and high delay in comparison with the direct component. Most of all, the presented results should be considered as reference (i.e. the best-case) measures calculated from experimental values obtained in the laboratory, under the most favorable conditions. Introduction of the multipath environment will cause interferences and the effect of frequency-selective fading that can be later included in a channel frequency response. It has been demonstrated, however, that the reflected ultrasonic signals in practice are relatively weak compared with the direct signal due to the directivity of the receiver [4] and that OFDM-based system with long symbols can efficiently cope with the interferences [4].

Atmospheric absorption of sound has been deeply investigated in the past and analytical formulas for the absorption coefficient have been given in the literature. We assume that f is the acoustic frequency in Hz, p_s is the atmospheric pressure, p_{s0} is the reference pressure (1 atm), T is the atmospheric temperature in K, and T_0 is the reference temperature (293.15 K). Based on formulas from [14], [17], the attenuation of ultrasound in the air can be calculated in dB as

$$L_{\text{atm}}(f,d) = -df^2 \left[1.6\times 10^{-10}\frac{p_{s0}}{p_s}\left(\frac{T}{T_0}\right)^{1/2} + \left(\frac{T_0}{T}\right)^{5/2} \times \left\{ 0.1107\frac{\exp(-2239.1/T)}{f_{r,O}+(f^2/f_{r,O})} + 0.9277\frac{\exp(-3352/T)}{f_{r,N}+(f^2/f_{r,N})} \right\} \right], \tag{2}$$

where $f_{r,O}$, $f_{r,N}$ (in Hz) are the relaxation frequencies of molecular oxygen and nitrogen given by Eq. (2),(3) in [17] that depend also on the absolute (h) and relative (h_r) humidity of the air, according to Eq. (4) in [17].

The acoustic field in front of the ultrasound transducer can be evaluated with a plane circular piston model [16]. The emitted field can be considered as the interference of a plane wave from the source and an edge wave diffracted at the transducer's aperture boundaries. This results in frequency-selective channel response with distinct zeros at frequencies dependent upon lateral displacement between the transmitter and receiver transducers [16]. However, when the ultrasonic transducers are aligned in parallel on the common axis, the spatial field response can be effectively described by a simpler model, as confirmed in experiments [18]. This model allows us to determine the theoretical, best-case performance limits of the airborne ultrasound channel. In the far-field the maximum sound pressure is always found on the axis [19] and the description by angular characteristic becomes appropriate.

It is also possible to extend the presented analysis to the near-field region by using one of the available time-domain propagation models [16], [20] that are also valid in the near-field. It must be noted, however, that in this region the directional pattern becomes distance-dependent. Moreover, deep fading at certain distances located on the acoustic axis will occur [19], [21] which degrades the system's reliability and makes the analysis much more complex. Due to considered area of application, i.e. the ultrasonic digital transmission at distances from 0.5 to 10 m, the near-field operation will not be discussed in this paper.

The far-field region extends for distances exceeding the Rayleigh distance: $R_0 = \pi D^2/(4\lambda)$, and for $d > R_0$ the inaccuracy of the far field approximation is lower than 3% [19]. The reduction of received signal power, resulting from beam divergence loss, may be evaluated based on the angle of divergence (eq. (4) in [18]), or more general – with Friis path loss formula [22] for the case of identical circular transmit and receive transducers:

$$L_{\text{spread}}(f,d) = 20\log\left[\frac{\varepsilon\pi D^2}{4\lambda d}\right] = 20\log\left[\frac{\varepsilon\pi f D^2}{4cd}\right], \quad (3)$$

where ε and D are the aperture efficiency and diameter, respectively, and c is the speed of sound in the air. In case of both mentioned methods, the received signal power is proportional to $[D^2/(\lambda d)]^2$ which is consistent with the general property of spherical spreading in the far field [21], and the difference is only in a constant ε associated with the transducers' efficiencies. This factor can be determined by calculations of the transducers' directivity or measured in laboratory experiments (later in this paper it will be included in P_{r}). From (3) we can see that the received signal level increases with the frequency due to rising directivity of the transducers, which partially compensates the attenuation in air (2).

In this work we have adopted frequency characteristics from [23], where overall system response (including the aperture efficiency factor) was measured for two different transducers: the commercial SensComp Series 600 [24] ($D = 38.4$ mm) and the laboratory-made prototype with high-k dielectric layer ($D = 10$ mm). The systems with these transducers offer the best performance in terms of the data rates achieved in ultrasonic transmission in air [13]. After compensating for attenuation (2), (3) introduced at the measurement distance (2 m and 0.5 m, respectively), we have estimated the normalized frequency characteristics $H_{\text{trans}}(f)$ of both transducers.

A. Parameters of channel frequency response

The frequency response of the considered channel, under the assumption of single-path LOS propagation in the far-field and axial placement of the transducers, and taking into account their frequency response $H_{\text{trans}}(f)$, can be approximated by

$$L_{\text{ch}}(f,d) = L_{\text{atm}}(f,d) + L_{\text{spread}}(f,d) + H_{\text{trans}}(f). \quad (4)$$

The plots of (4) as a function of frequency are shown in Fig. 1 for transmission distances up to 11 meters. During all calculations we assume climatic conditions as in [23]: $T = 20°$C, $r_h = 72\%$, $p_s = 1$ atm. The channel bandwidths, determined by a 6-dB drop, are marked with bold lines, and the attenuation of a lossy medium ($L_{\text{atm}}(f,d) + L_{\text{spread}}(f,d)$), irrespective of the transducers' characteristics, are shown with the dashed lines for the reference. We can clearly see that the channel bandwidth is shrinking with the increasing distance, and for the longest distances, only the narrow-band transmission may be employed.

We assume an AWGN background noise model as in [5], [6], [18] since no experimental data of frequency-dependent background noise is currently available for indoor airborne ultrasonic channels (apart from the severe interferences generated by industrial equipment [25], which is not a suitable environment for any acoustic communications). According to private communication with the author of [23], the background noise levels measured in the systems with both transducers (SensComp, high-k) were 3 mVpp and 0.45 mVpp, respectively (similar noise levels have been reported in [4], [5], [6],

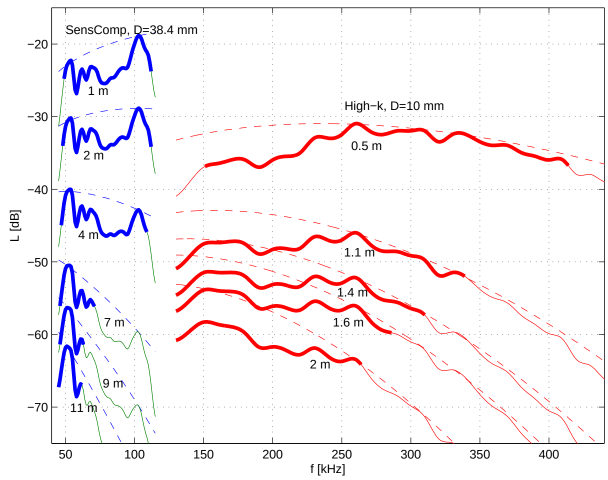

Fig. 1. Frequency response of the channel with different transducers

[18], [26]). The application of five-sigma rule to population of Gaussian samples allows us to estimate the noise variance σ^2. After dividing σ^2 by the system bandwidth (67 kHz and 220 kHz [23]) we obtain single-sided white noise power spectral densities for both systems: $N_0 = 2.68\times10^{-11}$ mW/Hz and $N_0 = 1.84 \times 10^{-13}$ mW/Hz, respectively. The received signals have been measured at the output of the low-noise amplifier (LNA) and the power values have been calculated for its output impedance ($Z_0 = 50\ \Omega$). This has no impact to our results since only relative power levels (SNR) are essential.

The power level of the transmitted signal was not reported in the literature and it needs to be estimated based on SNR values, e.g. from [23]. It is known that the transmitters emitted the fixed average power, regardless of the distance. In our work, the average power level P_{r} was calculated so that to achieve the nearest SNR values (in a least-square sense) to those reported in the literature for all the measured distances (see Tab. I in [23]), with respect to the system bandwidth and N_0 values from the previous paragraph, and under assumption of the flat spectrum of the transmitted signal. Finally, we have obtained $P_{\text{r}} = 9.8$ mW (SensComp) and $P_{\text{r}} = 0.15$ mW (high-k) The value of P_{r} should be considered as an extrapolation of the received signal power to $d = 0$ situation, that takes into account: the transmitted power level, the efficiency of the transducers and the gain of receiver LNA.

III. Performance Evaluation of Airborne Ultrasonic Channel

A. Theoretical capacity of the channel

The signals emitted in the high-data rate ultrasonic communication systems (e.g. [5], [18], [23]) can be considered as wide-band, since their bandwidths B are comparable with the center frequencies. Additionally, each of the transmitted frequency components is subjected to different attenuation level and the channel becomes frequency-selective that degrades simple estimations [13] based on the Shannon-Hartley theorem (1).

The channel with non-flat frequency response and frequency-dependent background noise can be approximated with a set of N parallel, narrow-band AWGN subchannels. In this case, the capacity is achieved [27] by choosing the power level p_n transmitted in each subchannel $(n = 1 \dots N)$ according to the water-filling principle [12]:

$$p_n = \begin{cases} K_d - A_{\text{ch}}(f,d)N_{\text{ch}}(f), & A_{\text{ch}}(f,d)N_{\text{ch}}(f) < K_d, \\ 0, & \text{otherwise}, \end{cases} \tag{5}$$

where $A_{\text{ch}}(f,d)$ is the frequency response (4) in a linear scale, $N_{\text{ch}}(f)$ is the noise power in a subchannel with the center frequency f and bandwidth Δ_f (for white noise we can assume: $N_{\text{ch}}(f) = N_0\Delta_f$), and K_d (*the water level*) is a constant associated with the total transmitted power

$$P = \sum_{n=1}^{N} p_n. \tag{6}$$

According to (5), more power is allocated to subchannels with higher SNR. The bandwidth occupation, resulting from non-zero power allocation (5), usually differs from a heuristic definition (e.g. based on 6 dB drop) [12]. The considered adaptive power allocation can be employed in ultrasonic communication systems with OFDM transmission, since in these systems the wide bandwidth is divided into subchannels with small sub-carrier spacing (e.g. $\Delta_f = 125$ Hz [4]).

B. Numerical evaluation of the channel capacity

The subchannel bandwidth Δ_f should be narrow enough to allow the assumption of locally-flat frequency response and noise p.s.d. The total bandwidth, for which frequency characteristics $H_{\text{trans}}(f)$ of the transducers were acquired, has been divided into subchannels with $\Delta_f = 1$ kHz. In case of the SensComp transducers, the differences of attenuation at subchannel boundaries have not exceeded 2 dB in most cases, and with high-k transducers, they are lower than 0.5 dB. Therefore, locally-flat channel assumption can be justified.

In order to determine the optimal power distribution (5), for each distance d, the water-filling procedure [12] has been performed in accordance with the flow chart shown in Fig. 2. The value of K_d has been iteratively increased with relative steps of 0.5%, starting from $\min\{A_{\text{ch}}(f,d)N_{\text{ch}}(f)\}$, and the resulting power distribution (5), (6) has been updated. The procedure has been terminated after the calculated power (6) has reached the fixed level P_{r} from the previous subsection. After that, the theoretical channel capacity for a given distance d has been calculated

$$C(d) = \Delta_f \sum_{n=1}^{N} \log_2 \left(1 + \frac{p_n}{N_0\Delta_f}\right). \tag{7}$$

It should be noted that in the case of frequency-dependent background noise model, the subchannel noise power $N_0\Delta_f$ has to be replaced with $N_{\text{ch}}(f)$. The optimal power distribution obtained with (5) for the systems with both types of transducers has been depicted in Fig. 3, and the channel capacity as a function of the distance under different climatic conditions T, h_r (for $p_s = 1$ atm) – in Fig. 4.

The obtained results show that the transmitted power is allocated in the bandwidth that reduces with increasing distance. For $d < 4$ m (SensComp transducers) or $d < 1$ m

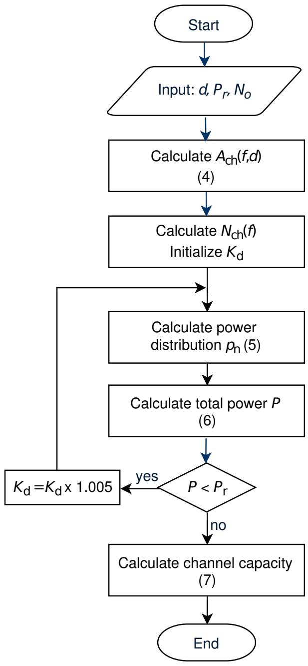

Fig. 2. Procedure of optimal power distribution

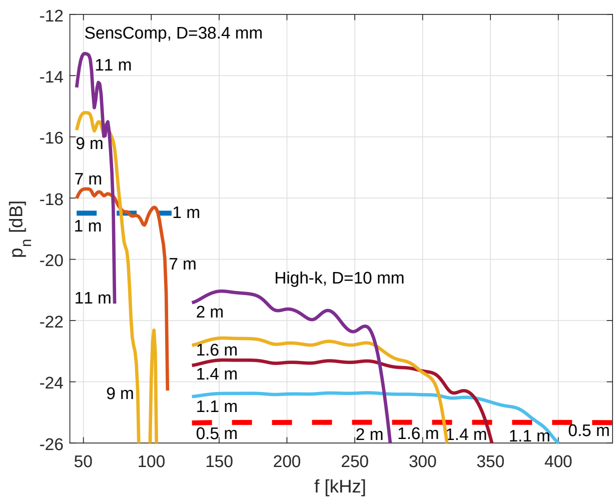

Fig. 3. Optimal distribution of transmitted power (dB relative to P_{r})

(high-k transducers), the power distribution is relatively flat over the entire available bandwidth (the shortest distances for both transducers: 0.5 m, 1 m have been distinguished with dashed lines in Fig. 3). For longer distances, however, the transmitted power is allocated only in the lowest frequency components. The narrow peak around 100 kHz is a result of water-filling procedure adaptation to the bimodal frequency response of the channel with SensComp transducers (see Fig. 1). In case of $d = 9$ m, the adaptation results in a discontinuous power distribution with zero-power region at $92 \dots 98$ kHz and non-zero power up to 105 kHz. For shorter distances ($d \leq 8$ m), the adaptation gives continuous power distribution with local minimum in the mentioned region, and for longer distances ($d \geq 10$ m), the obtained power distribution ends at frequencies below 80 kHz.

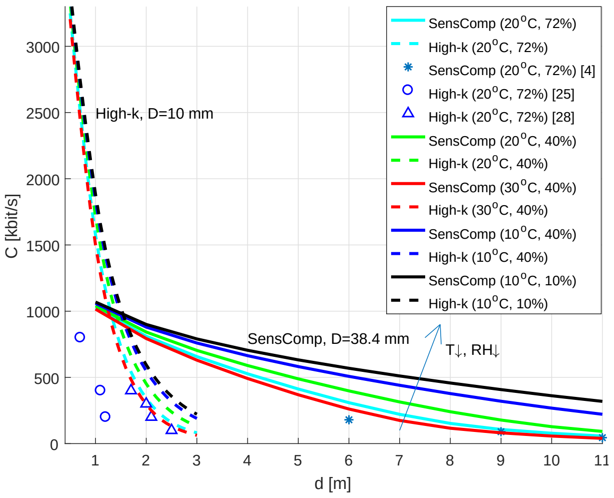

Fig. 4. Theoretical channel capacity for both types of transducers

We can observe a rapid fall of the channel capacity with the increasing distance due to severe atmospheric absorption of higher frequency components of ultrasound (2) and increasing path loss (3). For this reason, a reliable and fast ultrasonic communication over the distances longer than 11 m would be very hard to establish with practical limits on the emitted ultrasound pressure level [28]. The transmission with high data rates on the long distances, if necessary, could be performed only with using multiple-hop network topologies. It can be also noted that the channel capacity is higher for the system with high-k transducers ($D = 10$ mm) operating at short distances ($d < 1.5$ m) due to its wide band operation. At longer distances, however, the wide bandwidth does not improve the capacity due to severe attenuation of the signal resulting in low SNR.

The practical data rates achieved in the experimental systems [4], [23], [26] have been marked with stars, circles and triangles in Fig. 4 for the reference. It turns out that the experimental data rates from [4], [26] lie very close to the theoretical capacity limits derived for the same climatic conditions which suggests that near-optimal transmission setup has been employed in these systems. In the system described in [23], the sub-carriers were located from 200 to 400 kHz, which was only a part of the bandwidth available for the shortest distances (see Fig. 3). As a result, non-optimal power distribution took place and the obtained data rates (marked with circles) were lower than theoretical expectations.

The obtained theoretical limits suggests that in case of the shortest distances (i.e. $d < 1$ m for high-k, and $d < 5$ m for SensComp transducers), data rates higher than those reported in the experiments [4], [23], [26] may be obtained. For example, in the system with SensComp transducers, the data transfer rate was limited to 180 kbit/s due to design constraints [4], whereas the theoretical channel capacity is expected up to 1 Mbit/s. For the same reason, the data rate in the system with high-k transducers was limited to 400 kbit/s [26] or 800 kbit/s [23], while the theoretical channel capacity at the shortest distances is expected up to 3 Mbit/s. Therefore, further development of short-range airborne ultrasonic communication systems is still necessary.

The capacity plots from Fig. 4 can be approximated by

$$C(d') \approx C_0 \times \log_2(1 + C_1 \times 10^6 \times 10^{-d' C_2/100} d'^{-2}) \quad (8)$$

in kbit/s, where $d' = d/D$ is the normalized distance. The parameters C_0, C_1, C_2 can be numerically calculated from three selected points of the initial part of the plot ($d' < 105$) for which SNR $\gg 1$. The approximation (8) can predict the channel capacity for $d < 6.5$ m (SensComp) or $d < 1.1$ m (high-k transducers) with accuracy better than 5%. For greater d, it underestimates the channel capacity which results in diminished accuracy. The values of C_0, C_1, C_2 have been summarized in Tab. I for both types of transducers.

TABLE I
PARAMETERS OF APPROXIMATION (8) FOR SELECTED T, h_r ($p_s = 1$ ATM)

	20°C, 72%	20°C, 40%	10°C, 40%	30°C, 40%
SensComp:				
C_0	70.0	71.6	68.1	71.4
C_1	36.0	26.9	49.5	27.7
C_2	1.22	0.88	0.71	1.28
High-k:				
C_0	470.6	441.3	415.6	431.4
C_1	0.88	1.47	2.43	1.76
C_2	0.94	1.00	1.06	1.22

C. Impact of climatic conditions to the channel capacity

During this analysis, we assume that the transducer frequency response $H_{\text{trans}}(f)$ does not depend on the climatic conditions. The transducer response is typically described by a plane piston model [16], [20] and formulas that involve diameter of the aperture (D) and the speed of sound in the air (c). The value of c depends mostly on the temperature and changes by $\pm 2.6\%$ for $T = 25 \pm 15$°C. The changes of D due to thermal expansion are expected about $\pm 0.02\%$ for the same range of T, assuming gold foil as the working material [24]. Therefore, the variations of c, D that impact the transducer response are negligible in the considered range of climatic conditions since they are much lower than the influence of the transmission medium at distances changing from 0.5 to 10 m (see Fig. 1).

However, when (2) is taken into account, the ultrasonic channel response (4) and therefore the theoretical channel capacity becomes climatic-dependent. This dependency is especially noticeable for longer distances, as the plots for different values of T, h_r diverge in Fig. 4. Higher channel capacity can be expected for lower air temperature and lower relative humidity. The dependencies of the channel capacity on T and h_r have been illustrated in Fig. 5 and Fig. 6, respectively, for the systems with two types of transducers and for different distances d.

The theoretical channel capacity also depends on the atmospheric pressure (p_s), as shown in Fig. 7 – it increases with p_s rising from 750 hPa to 1040 hPa. That dependency is clearly visible for the wide-band transducer (high-k), even at the smallest distances (d =1 m).

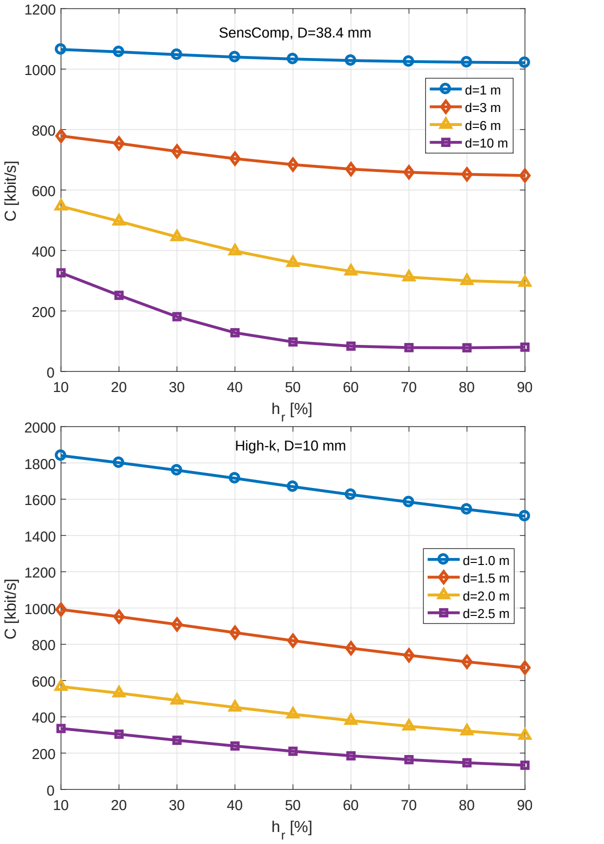

Fig. 6. Theoretical channel capacity as a function of relative humidity ($T = 20°\text{C}$, $p_s = 1$ atm)

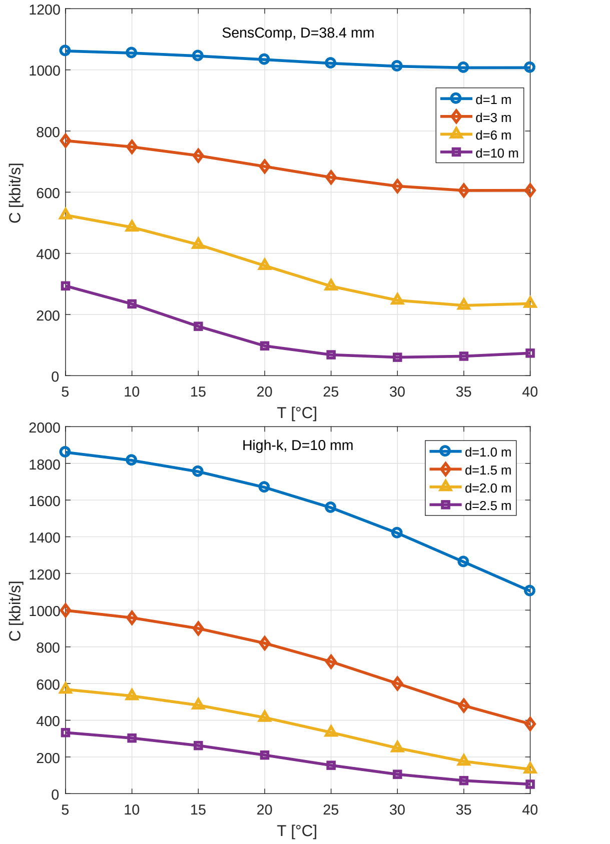

Fig. 5. Theoretical channel capacity as a function of temperature ($h_r = 50\%$, $p_s = 1$ atm)

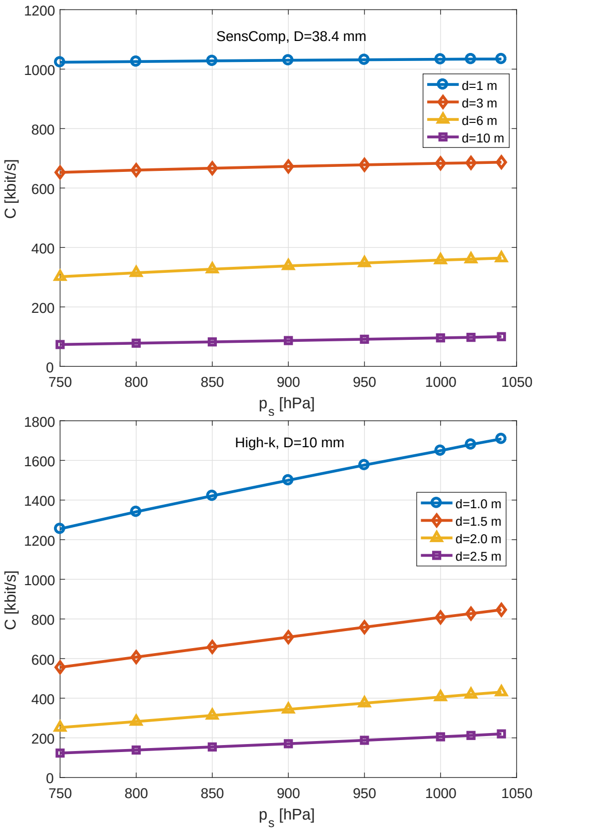

Fig. 7. Theoretical channel capacity as a function of atmospheric pressure ($T = 20°\text{C}$, $h_r = 50\%$)

IV. CONCLUSIONS

In this paper we have applied frequency-dependent channel model, based on well-known sound attenuation effects, to the airborne ultrasound transmission channel. Numerical parameters of the model have been adopted from experimental results available in the literature. This approach allows us to numerically evaluate the channel theoretical capacity for any distance in the far field, without limitation to the points with experimentally determined SNR measures. It turns out that in short distances it may be possible to achieve higher data transfer rates than those obtained with experimental systems described in the literature [4], [23], [26].

Because of well-described influence of the air temperature, pressure and relative humidity to the attenuation of acoustic and ultrasonic waves in the air, it is also possible to extend the theoretical predictions to climatic conditions different from these recorded in the experiments. The theoretical analysis shows that the channel capacity rises with the falling air temperature and relative humidity. In spite of negligible impact at the shortest distances (e.g. $d = 1$ m), this relation becomes more and more visible as the distance increases. The influence of the atmospheric pressure has been also investigated; however, it has lower impact to the channel capacity when compared to the air temperature and humidity, and it is mostly observed in the case of wide-band (high-k) transducers.

REFERENCES

[1] F. J. Canete, J. López-Fernández, C. García-Corrales, A. Sánchez, E. Robles, F. J. Rodrigo, and J. F. Paris, "Measurement and modeling of narrowband channels for ultrasonic underwater communications," *Sensors*, vol. 16, no. 2, p. 256, Feb 2016. [Online]. Available: http://www.mdpi.com/1424-8220/16/2/256

[2] T. J. Lawry, K. R. Wilt, J. D. Ashdown, H. A. Scarton, and G. J. Saulnier, "A high-performance ultrasonic system for the simultaneous transmission of data and power through solid metal barriers," *IEEE Transactions on Ultrasonics, Ferroelectrics, and Frequency Control*, vol. 60, no. 1, pp. 194–203, January 2013.

[3] D. Ma, Y. Shi, W. Zhang, and G. Liu, "Design of acoustic transmission along drill strings for logging while drilling data based on adaptive NC-OFDM," *AEU - International Journal of Electronics and Communications*, vol. 83, pp. 329 – 338, 2018.

[4] W. Jiang and W. M. D. Wright, "Evaluation of multiple-channel OFDM based airborne ultrasonic communications," *Ultrasonics*, vol. 71, pp. 288–296, 2016.

[5] C. Li, D. A. Hutchins, and R. J. Green, "Short-range ultrasonic communications in air using quadrature modulation," *IEEE Transactions on Ultrasonics, Ferroelectrics, and Frequency Control*, vol. 56, no. 10, pp. 2060–2072, October 2009.

[6] ——, "Short-range ultrasonic digital communications in air," *IEEE Transactions on Ultrasonics, Ferroelectrics, and Frequency Control*, vol. 55, no. 4, pp. 908–918, April 2008.

[7] G. E. Santagati and T. Melodia, "A software-defined ultrasonic networking framework for wearable devices," *IEEE/ACM Transactions on Networking*, vol. 25, no. 2, pp. 960–973, April 2017.

[8] C. E. Shannon, "Communication in the presence of noise," *Proceedings of the IRE*, vol. 37, no. 1, pp. 10–21, Jan 1949.

[9] R. A. Primerano, "High bit-rate digital communication through metal channels," Ph.D. dissertation, Drexel University, July 2010.

[10] J. D. Ashdown, G. J. Saulnier, T. J. Lawry, K. R. Wilt, and H. A. Scarton, "High-rate ultrasonic communication through metallic barriers using MIMO-OFDM techniques," in *MILCOM 2012 - 2012 IEEE Military Communications Conference*, Oct 2012, pp. 1–6.

[11] L. Galluccio, T. Melodia, S. Palazzo, and G. E. Santagati, "Challenges and implications of using ultrasonic communications in intra-body area networks," in *2012 9th Annual Conference on Wireless On-Demand Network Systems and Services (WONS)*, Jan 2012, pp. 182–189.

[12] M. Stojanovic, "On the relationship between capacity and distance in an underwater acoustic communication channel," *SIGMOBILE Mob. Comput. Commun. Rev.*, vol. 11, no. 4, pp. 34–43, Oct. 2007. [Online]. Available: http://doi.acm.org/10.1145/1347364.1347373

[13] G. Mazurek, "Channel capacity of short-range ultrasonic communications in air," *IEEE Communications Letters*, vol. 22, no. 1, pp. 117–120, Jan 2018.

[14] H. E. Bass, L. C. Sutherland, A. J. Zuckerwar, D. T. Blackstock, and D. M. Hester, "Atmospheric absorption of sound: Further developments," *The Journal of the Acoustical Society of America*, vol. 97, no. 1, pp. 680–683, 1995.

[15] G. Mazurek, "Basic channel parameters of ultrasound transmission in air," in *2018 22nd International Microwave and Radar Conference (MIKON)*, May 2018, pp. 607–609.

[16] C. Li, D. A. Hutchins, and R. J. Green, "Response of an ultrasonic communication channel in air," *IET Communications*, vol. 6, no. 3, pp. 335–343, February 2012.

[17] H. E. Bass, L. C. Sutherland, and A. J. Zuckerwar, "Atmospheric absorption of sound: Update," *The Journal of the Acoustical Society of America*, vol. 88, no. 4, pp. 2019–2021, 1990.

[18] W. Jiang and W. M. D. Wright, "Multichannel ultrasonic data communications in air using range-dependent modulation schemes," *IEEE Transactions on Ultrasonics, Ferroelectrics, and Frequency Control*, vol. 63, no. 1, pp. 147–155, Jan 2016.

[19] J. Krautkrämer and H. Krautkrämer, *Ultrasonic Testing of Materials*, 4th ed. Springer Berlin Heidelberg, 1990.

[20] J. Li and B. Piwakowski, "A time-domain model and experimental validation of the acoustic field radiated by air-coupled transducers," *Ultrasonics*, vol. 82, pp. 114–129, 2018.

[21] J. H. Ginsberg, *Acoustics – A Textbook for Engineers and Physicists. Volume II: Applications*. Cham, Switzerland: Springer International Publishing AG, 2018.

[22] H. T. Friis, "A note on a simple transmission formula," *Proceedings of the IRE*, vol. 34, no. 5, pp. 254–256, May 1946.

[23] W. Jiang and W. M. D. Wright, "Indoor airborne ultrasonic wireless communication using OFDM methods," *IEEE Transactions on Ultrasonics, Ferroelectrics, and Frequency Control*, vol. 64, no. 9, pp. 1345–1353, Sept 2017.

[24] SensComp, Inc., *Series 600 environmental grade ultrasonic sensor*. Available: http://www.senscomp.com/pdfs/series-600-envir-grade-ultrasonic-sensor-spec.pdf: Accessed on Sep. 27, 2017. [Online], 2015.

[25] H. E. Bass and L. N. Bolen, "Ultrasonic background noise in industrial environments," *Journal of The Acoustical Society of America*, vol. 78, pp. 2013–2016, 12 1985.

[26] W. Jiang and W. M. D. Wright, "Full-duplex airborne ultrasonic data communication using a pilot-aided QAM-OFDM modulation scheme," *IEEE Transactions on Ultrasonics, Ferroelectrics, and Frequency Control*, vol. 63, no. 8, pp. 1177–1185, Aug 2016.

[27] R. G. Gallager, *Information Theory and Reliable Communication*. New York: J. Wiley, 1968.

[28] T. Toivo, P. Orreveteläinen, S. Kännälä, and T. Toivonen, *Survey on limiting exposure to ultrasound (STUK-TR26)*. Helsinki, Finland: Radiation and Nuclear Safety Authority, June 2017.